

# PLASTIC STRAIN BASED CRITERION FOR FAILURE PREDICTIONS OF SHORT FIBER REINFORCED PLASTICS AT STRUCTURAL LEVEL

*Maxime A. Melchior, Thierry Malo  
e-Xstream engineering, an MSC Software Company*

*Zhenyu ZHANG, Alan WEDGEWOOD, Mattia SULMONI  
DuPont*

## Abstract

Failure modeling of short fiber reinforced plastics (SFRP) is a key challenge to obtain accurate predictions on crash applications. Composite are considered as SFRP when the fiber aspect ratio ranges between 15 and 35. One of their specificities is that the orientation varies locally. Therefore, accuracy at part level requires a material model which is predictive for any strain rate, loading case and/or fiber orientation. The model is typically calibrated on tensile tests at three different angles and three different strain rates.

A new failure package based solely on a triaxiality dependent plastic strain-based failure criteria at the matrix level has been developed in Digimat<sup>®</sup>. The new failure package contains the definition of the criteria in the mean-field approach as well as new failure criteria in our Hybrid solution. The Hybrid solution is a robust, fast and easy reduced model built on the top of the mean-field homogenization which is designed specifically for crash applications in order to provide accurate predictions in an industrial time frame.

The developed tools are presented and the achieved results compared to experimental data on an injected beam with a Zytel<sup>®</sup> PA66GF30 composite produced by DuPont<sup>®</sup>. The paper covers model calibration, its validation at dumbbell level and predictions on the structural application.

## Introduction

Composites are increasingly being used in structural automotive parts, both chopped FRPs as well as CFRPs more traditionally used in the aerospace industry. This heightens the demand for accurate simulation tools to predict structural performances. Failure is a key performance which needs to be accurately predicted in order to help an engineer to design their part such that weight saving is maximum.

Numerous process simulation codes can compute fiber orientation resulting from the manufacturing process such as injection molding, drape molding, compression molding and resin transfer molding. The microstructure determines the anisotropic character of the material. By interfacing with processing data as well as structural FEA codes, Digimat<sup>®</sup> software bridges the gap between the process and the structural part performances, offering multi-scale material modeling tools capable of modeling the anisotropic, nonlinear, strain-rate dependent and other specificities of composites in FEA.

The purpose of this paper is to illustrate how multi-scale material modeling can be applied to obtain accurate failure modeling solution for composites. This paper describes how the SFRP behavior can be modeled thanks to micromechanics and the failure models developed in Digimat<sup>®</sup> by e-Xstream engineering. The main focus is on the procedure to be used to ensure that an experimental campaign can be successfully transformed into an accurate material model. Finally, it addresses the ability to exploit corresponding material models in the framework of multi-scale structural simulations.

# Mean-field homogenization of short fiber reinforced plastics

## Mean-Field Homogenization Theory

Composites are by definition a combination of two or more constituents to obtain an improved material in comparison to the base constituents. As composite properties depend on the material microstructure including fiber amount and orientation, they are adequately modeled from micromechanics. In particular, mean-field homogenization combines the properties of the underlying constituents of a multi-phase material so that the original heterogeneous material is represented by an equivalent homogeneous one. Implemented in the Digimat software [1], this technology has proven effective for a broad range of materials.

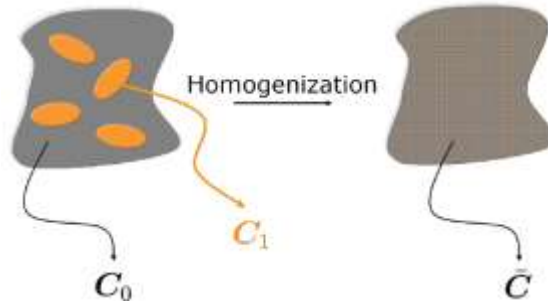


Figure 1: Heterogeneous material (left) from which its equivalent stiffness  $\bar{C}$  is computed from homogenization.

## Application to short fiber reinforced plastics

The specificity of short fiber reinforced plastics is that the material model should be accurate for any orientation tensor. The composite orientation tensor is represented by a set of pseudo-grains having a fixed orientation and a given weight computed such that weighted average of all fixed orientations equals the orientation tensor [2]. The behavior of a composite is then obtained in two steps. The behavior of each pseudo-grain is computed from the matrix and fiber behavior. The composite behavior is then obtained from averaging the behavior of each pseudo-grain [3].

## Failure of short fiber reinforced plastics

In the scope of this paper, two failure criteria are compared. The first one is a Tsai-Hill 3D transversely isotropic criteria applied at the pseudo-grain level [4]. The composite is considered as failed when the average failure indicator reaches a critical value. This failure criteria offers the perfect solution for customers that possess a small amount of experimental data since only three parameters are required. Although the prediction of the failure criteria has a good agreement with experimental data for a particular load case [5], accuracy for any type of loading depends on the failure envelope designed by Tsai on continuous fiber composite.

The second criteria is a triaxiality dependent plastic strain based failure criteria applied the matrix phase level. Improved failure predictions using a triaxiality failure model applied at the composites level were demonstrated using an uncoupled Digimat® with Abaqus approach [6]. Development of a fully coupled Digimat® triaxiality based failure criteria at the matrix phase level by e-Xstream engineering further expands upon this failure modeling capability, while also making it more accessible and easier to use. This failure model parameters are couples between triaxiality and critical accumulated plastic strain in the matrix phase. Customer should define enough couples to ensure the failure is well modeled for the range of triaxiality values experienced by the tested component. The accuracy of this failure criteria will rely on the accuracy of the prediction of the accumulated plastic strain and of the triaxiality in the matrix.

While it is known that the accumulated plastic strain is globally well predicted even if slightly underestimated by the mean-field homogenization model, the predictions of the triaxiality has never been investigated. Mean-field triaxiality predictions have been compared to full-field results using a unit cell of perfectly aligned fibers loaded in tension at various angle. The results on the Figure 2 shows that triaxiality trends per loading angles are captured as well as their evolution with macroscopic pseudo-grain strain. The main difference are at 0° and 15° where mean-field homogenization overestimates by about 10% the triaxiality predicted with respect to the full-field homogenization.

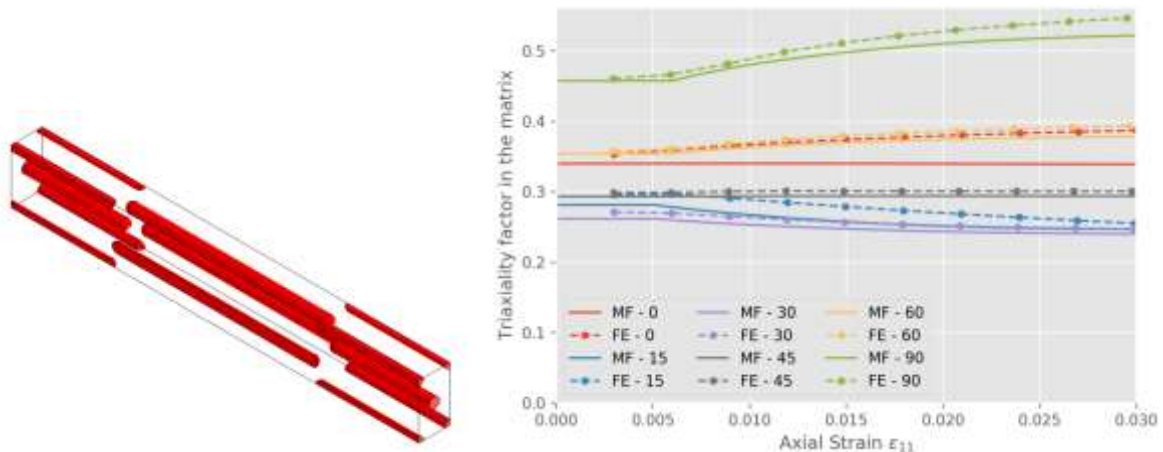


Figure 2 : Comparison of the evolution of the triaxiality with the strain between mean-field and full-field homogenization for tensile at different angle ranging from 0 to 90° on a unit cell of aligned orientation.

## From experimental data to accurate failure predictions at structural level

### Experimental data

The geometry specimen is a dumbbell shape, described by test standards like the ASTM D638, ISO 527 and ISO 8256, cut out of an injection molded plaque. The dumbbells are cut in different angle from the resin flow in order to identify the anisotropy of the material. They are mainly loaded in tension and sometimes in bending. Injection molded plaques typically display a gradient of orientation through the thickness, that needs to be accounted for in the modeling to accurately predict part response both in terms of stiffness and failure. Several replicates in each direction are needed in order to determine the average behavior.

### Calibration procedure

The calibration is done following two steps. The first one is the calibration of the stiffness properties, while the second step involves calibration of the failure criteria.

Customers targeting quasi-static analysis, an automated reverse engineering tool does both steps for you in a single click. The per-phase behavior, the aspect ratio and the microstructure, in case this last one is not provided by the customer, are reverse engineered. The automated reverse engineering draws upon the best practices and the experience of e-Xstream.

For dynamic analysis, an interactive reverse engineering procedure allows the user to separately calibrate the stiffness and a strain rate dependent failure. The interactive reverse engineering procedure can also be used to fine tune the parameters of the material model obtained by the automated reverse engineering tool.

The stiffness calibration procedure consists of simultaneously calibrating the matrix Young's Modulus, the hardening parameters and the viscous function, as well as the fiber aspect ratio, from the tensile data measured at different angles and at different strain rates.. The strain rate dependent failure calibration is performed for each strain rate. The failure calibration takes the specimen geometry into account in order to extract the local strain at break. The latter can also be obtained through Digital Image Correlation (DIC).

## **Model reduction**

The result of the calibration is a material model that performs mean-field homogenization to predict the composite behavior. A direct use of the material model leads to prohibitive simulation time for a typical customer application. A model reduction is therefore performed prior to the structural simulation. This reduction only has to be done once for a material model.

The reduced model is a macroscopic model which is calibrated thanks through virtual experimental tests performed with mean-field homogenization [7]. The obtained model is matching the mean-field homogenization results for all standard configurations of microstructure and loadings.

## **Validation**

The reduced model is then tested by FEA simulation of the experimental data from which is was calibrated. Additional tests can be added in order increase the confidence in the material model. Dumbbell simulations are typically run with implicit FEA code and solid elements.

In order to assess the final failure of such specimen, a progressive failure model can be added to capture damage propagation at this scale. Several damage laws are proposed: Instantaneous, Linear or Exponential. The latter one allow to control the strain between failure initiation and final failure as well as the stiffness loss rate with respect to strain. The Linear law allows only the control of the strain between failure initiation and final failure and enforces a linear relationship. The Instantaneous law enforces a small strain between failure initiation and final failure and a linear slope. The last one is dedicated to SFRP grades which often exhibit instantaneous damage after failure initiation while the others are most likely used to capture larger fracture toughness when significant plasticity prior final breakage from failure initiation is identified. The exponential damage law even allows to minimize quick damage propagation due to numerical concentration by limiting load redistribution to surrounding elements.

## **Structural application**

Running a structural application requires mapping of the manufacturing data from the injection mesh to the simulation mesh. The standard procedure takes into account local fiber orientation in the structure, though other factors can also be accounted for, such as the initial stress, weld lines, local porosity, local aspect ratio and fiber volume fraction variation. Manufacturing data can be mapped from solid injection mesh to solid and shell structural mesh as well as from shell injection mesh to shell structural mesh.

The material response at each integration point is then computed using the reduced model for the local orientation, porosity, aspect ratio or volume fraction. Regarding failure, a knock-down factor can be applied to take the influence of the weld line and of the local porosity.

## Application on an injected beam with a Zytel® PA66GF30 composite produced by DuPont

### Experimental campaign

#### *Dogbone Tension Test*

Short fiber reinforced composite plaques are manufactured by injection molding a thermoplastic polymer compounded with short glass fiber into a 125 mm x 125mm x 3mm plaque. Dogbone shaped coupons are cut from the plaque at three different angles, 0°, 45°, and 90°, with respect to the primary flow direction as shown in Figure 3. These samples are then conditioned to achieve equilibrium moisture content at 23°C and 50% RH. High rate tensile tests with different loading speeds are conducted using state of the art testing capabilities shown in Figure 4. The processed stress-strain curves at three angles with strain rates ranging from  $0.001\text{s}^{-1}$  to  $100\text{ s}^{-1}$  are summarized in Figure 5. The curves are trimmed at the maximum stress after which the specimen is considered to be completely broken and the stress abruptly plummets to zero. The material behavior is anisotropic and rate dependent. Because short fibers are more aligned in the flow direction, the stiffness at 0° is higher than the stiffness at the other two angles. As the strain rate increases, stress at break increases while the strain at break decreases.



Figure 3 : Samples at coupon level are cut from injection molded plaque at 0°, 45°, and 90°

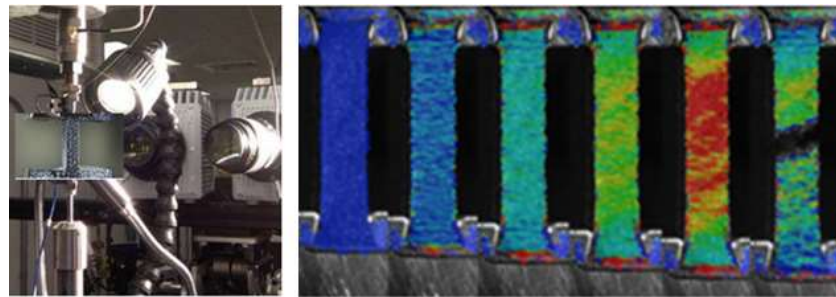


Figure 4 : High strain rate data measured using a high rate test frame, high speed cameras and data acquisition system. Strain was determined using a digital image correlation system.

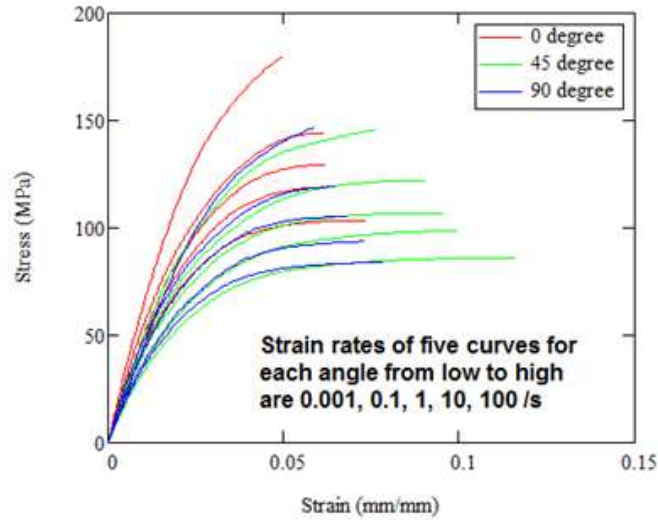


Figure 5 : Stress-strain curves as a function of strain rate and sample angle for short fiber composites.

### Chopped Fiber Orientation

Accurate representation of fiber orientation is essential in developing an anisotropic material model for short glass reinforced materials. The orientation is estimated by duplicating the injection molding process with a mold filling analysis using Autodesk Moldflow® Folgar-Tucker mid-plane model with  $C_i = 0.0023$  and  $D_z = 0.1412$ . The resulting fiber orientation distribution is mapped onto the structural shell mesh of the dog-bone specimen using as illustrated in Figure 6.

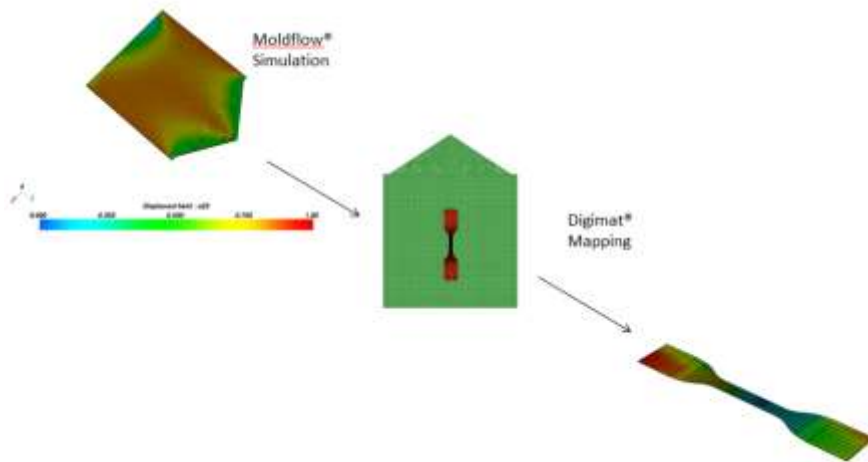


Figure 6. Fiber orientation from a mold filling analysis of an injection molded plaque is transferred to the dog-bone-specimen.

To check the accuracy of the mold filling simulation fiber orientation prediction, an experimental determination of the fiber orientation tensor through the thickness at the center of the plaque was done by extracting the orientation from computerized tomography scans. In Figure 7, a comparison is made at the plaque’s center, between experimentally determined 2nd order orientation tensor values and those predicted by the mold filling simulation. The simulation

prediction captures the trend of orientation variance from specimen skin to core. The comparison shows good agreement, lending confidence to the application of the mold filling simulation to predict the orientation values for the entire plaque.

### Structural Beam Flexure Test

Structural beams with the geometry of 730mm in length and 140mm in width are manufactured by injection molding process. All four injection ports along the length of the beam are opened at the same time, as shown in Figure 8. The injection flow meets at the middle of the beam forming a weld line at the middle. The injected beams are conditioned to reach the equilibrium moisture content at 23°C and 50% RH.

The beam is placed on two supports and loaded by an impact nose as shown in Figure 8. The loading nose is driven with constant speed control. The force and the displacement of the loading nose are measured. A video of the test and pictures of the failed sample are recorded. These data are used to estimate the model capability in the following sections.

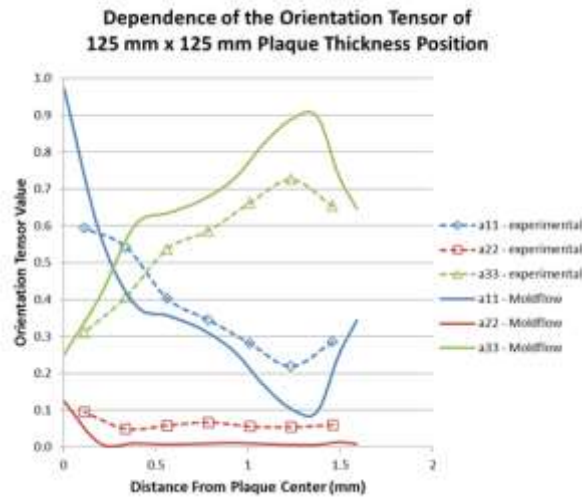


Figure 7. Experimental and mold filling simulation predicted principal values of the 2nd order orientation tensor are compared for half of the plaque thickness. The tensor directions are: 11 -perpendicular to the injection flow, 22 - plaques thickness, and 33 - injection flow direction. Symmetry of the experimental orientation about the plaque center is assumed.

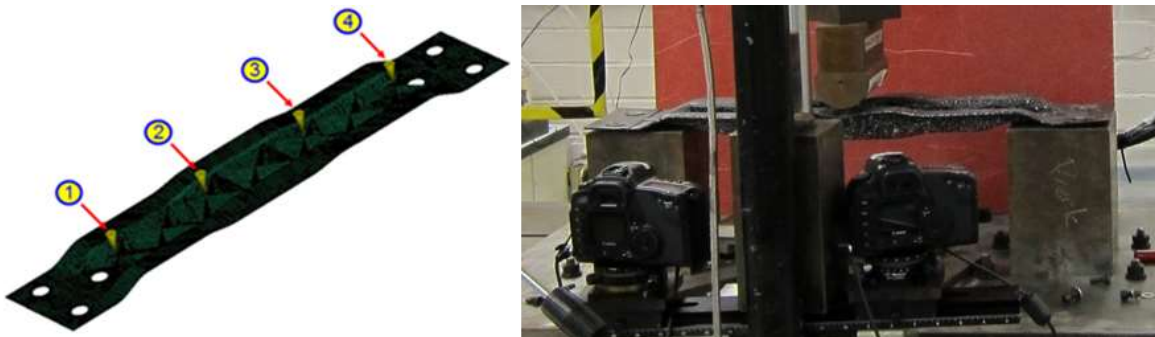


Figure 8 : Injection gate location of structural beam (left) and structural beam flexure test set up (right)

## Calibrated material model

Two material models have been calibrated. The non-linear behavior is the same in both models, only the failure models are different. The matrix has been modeled as elasto-viscoplastic while the fibers are considered to be elastic. The first failure model is the Tsai-Hill 3D transversely isotropic applied at the pseudo-grain level. The second failure model is the critical accumulated plastic strain criteria applied at the matrix level.

The calibrated material model response is shown on the Figure 9 for the three strain rates tested in tension at 0, 45 and 90°. The model captures the strain rate sensitivity of both the stiffness and the failure for both failure models. The main discrepancy is due to the use of an elasto-viscoplastic plastic model while the experimental data shows a viscoelastic-viscoplastic behavior.

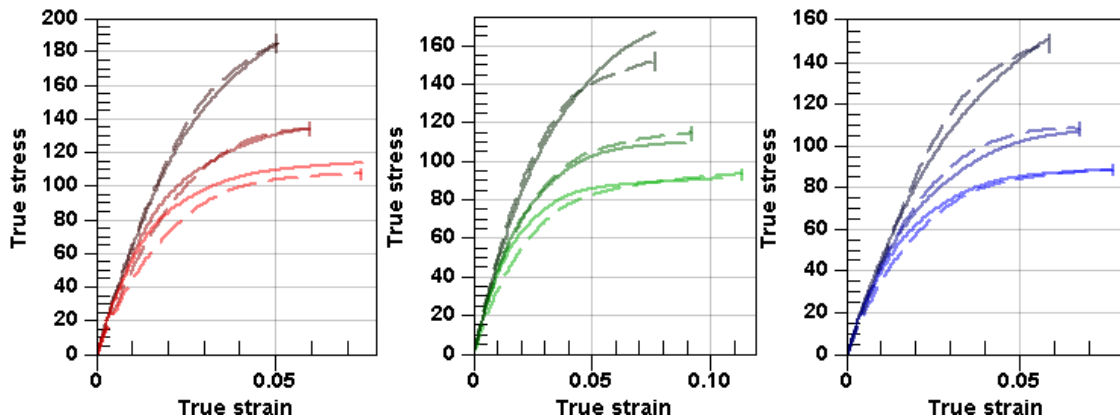


Figure 9 : Comparison between experimental data and Digimat model with Tsai-Hill 3D Transversely Isotropic failure criteria for three strain rates (0.001, 1 and 100 s<sup>-1</sup>) and for three loadings (0° in red, 45° in green and 90° in blue). Experimental data are in dotted line and material model in straight line.

The average error on the failure strain at break is of 2.5% with a maximum error of 7% on the strain at break at 45° for the quasi-static strain rate as shown on Table 1.

Table 1 : Comparison between experimental and Digimat model with Tsai-Hill 3D Transversely Isotropic failure criteria strain at break for three loadings and three strain rate.

Angle (°)	Strain rate (s <sup>-1</sup> )	Experimental	Digimat	Error (%)
0	0.001	0.0739	0.0742	0.4
0	1	0.0597	0.0595	-0.3
0	100	0.0502	0.0505	0.6
45	0.001	0.1132	0.1053	-7.0
45	1	0.0921	0.0894	-2.9
45	100	0.0765	0.077	0.7
90	0.001	0.0766	0.0765	-0.1
90	1	0.0672	0.0668	-0.6
90	100	0.0583	0.0578	-0.9
Global				-2.5



The material model using the triaxiality based critical accumulated plastic strain failure criteria perfectly matches the experimental strain at break. Each experimental test defines a specific couple of critical accumulated plastic strain versus triaxiality. This identification leads to the definition of three couples for which the triaxiality ranges between 0.33 and 0.5. Three other couples are added at triaxiality  $-1/3$ , 0 and  $2/3$ , in order to cover a wide range of triaxiality. The critical accumulated plastic strain used at these triaxiality values are multiples of the maximum critical accumulated plastic strain observed for the three tensile tests. Multiplication factors of 5, 3 and 1, respectively, have been chosen based on the experience gathered at e-Xstream. A weakness of the calibrated failure model is that it leads to a sharp drop (Figure 10).

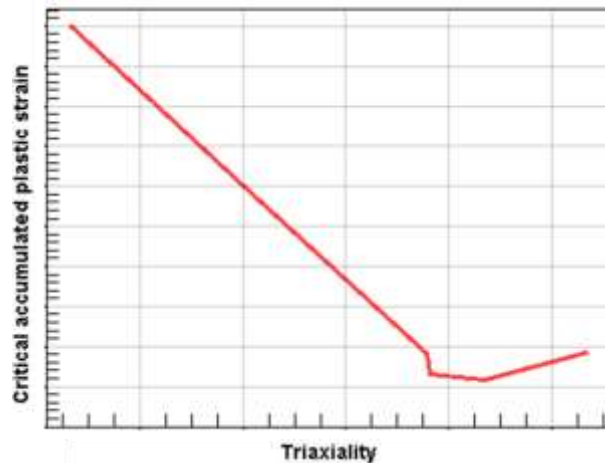


Figure 10 : Calibrated triaxiality based critical accumulated plastic strain criteria

## Validation

A first validation step consists of comparing the reduced model with the mean-field homogenization model. The comparison is shown for tensile and shear loading for four orientations for two strain rates for the material model with the Tsai-Hill 3D transversely isotropic failure criteria on Figure 11. The reduced model shows a good match with the mean-field homogenization technique. The main discrepancy is on the transverse behavior of the fully aligned orientation in tensile and in shear.

The comparison is shown for tensile and shear loading at the strain rate  $0.001s^{-1}$  for the triaxiality based critical accumulated plastic strain on Figure 12. The reduced model showed a good match with the mean-field homogenization technique. The main discrepancy is on the transverse prediction of the aligned orientation for the break strain is twice the mean-field homogenization model value.

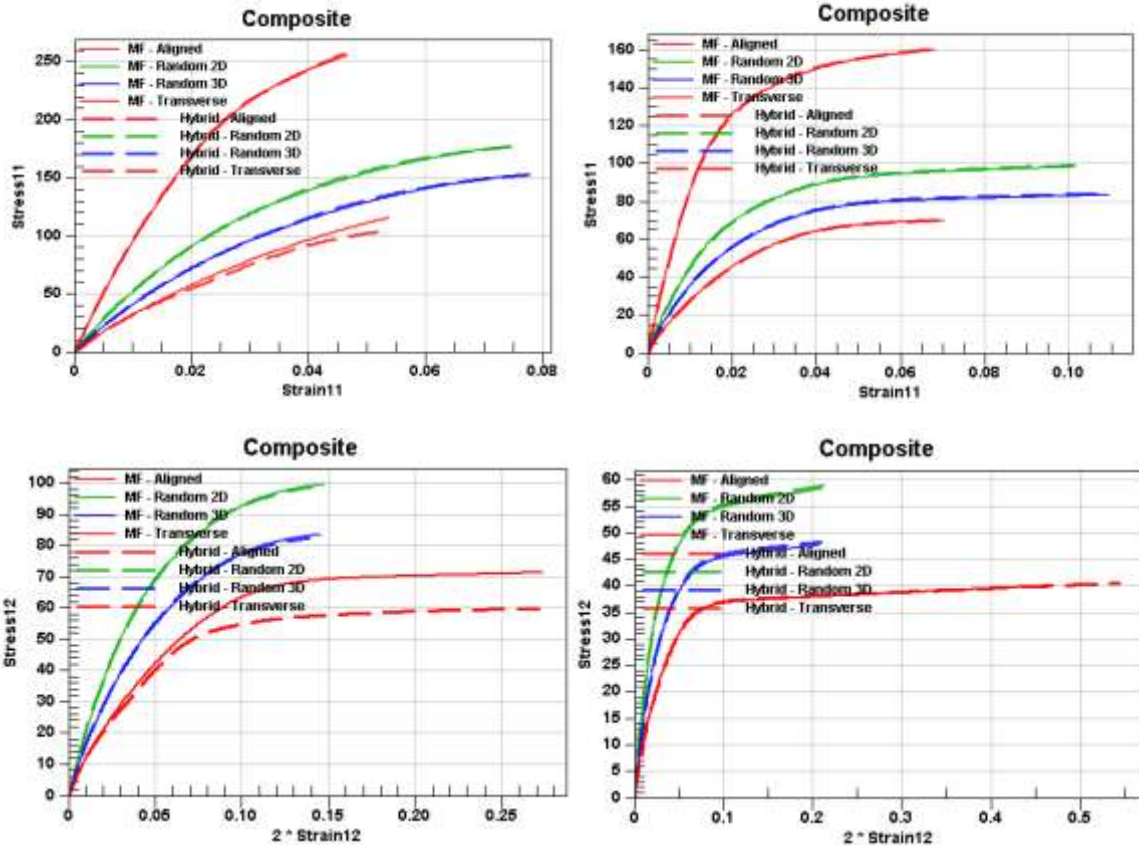


Figure 11 : Comparison between the mean-field homogenization model (MF) and the reduced model (Hybrid) for four loadings cases : (top-left) tensile test at  $100 \text{ s}^{-1}$ , (top-right) tensile test at  $0.001 \text{ s}^{-1}$ , (bottom-left), shear test at  $100 \text{ s}^{-1}$  and (bottom-right) shear test at  $0.001 \text{ s}^{-1}$ .

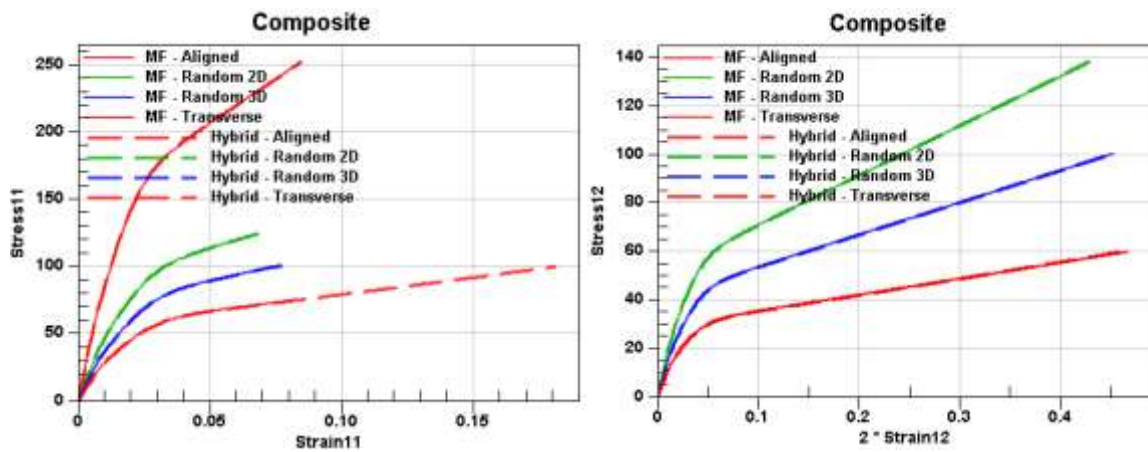


Figure 12 : Comparison between the mean-field homogenization model (MF) and the reduced model (Hybrid) for four loadings cases : (left) tensile test at  $0.001 \text{ s}^{-1}$  and (right) shear test at  $0.001 \text{ s}^{-1}$ .

# Structural application

## CAE Model Setup

A constant velocity of 0.127 m/s is applied on the impact nose to simulate a dynamic three-point flexure test. A friction type of contact is defined between the beam and the impactor. A Moldflow® analysis is conducted to simulate the injection molding process and to obtain the fiber orientation distribution across the beam. The reaction force and displacement of the impact nose from FEA are collected at high frequency to compare with experimental data.

## Results

The results obtained with the two material models are compared to the experimental data on Figure 13. The linear and non-linear behavior is correctly captured by the models until 20mm of displacement. A small difference appears between 20mm and 30mm before any failure event without reasonable explanation so far. With the Tsai-Hill failure criteria predicts a first failure event occurs around 30mm and a more significant event appears around 35mm while the experimental data only show a significant even around 40mm. With the triaxiality based critical accumulated plastic strain failure criteria, a first failure event occurs around 35mm and a second event appears around 37mm. The overall behavior of the results with the latter criteria is close to the experimental test.

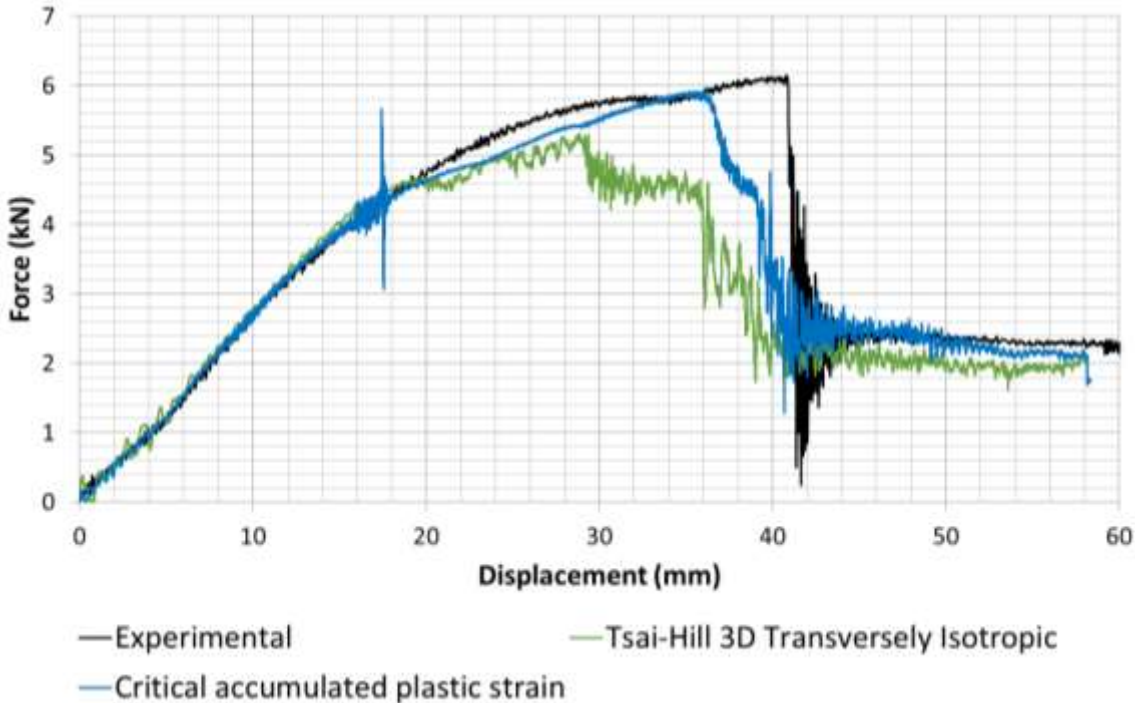


Figure 13 : Comparison of two material models differentiated by their failure model with experimental data

## Conclusions

Today, the design of high quality, light and energy efficient vehicles is crucial for success in the automotive industry. Optimal designs suited for this new environment can be achieved using predictive CAE and advanced material modeling tools. This paper presents a workflow to accurately predict failure of short fiber reinforced plastics composite structures implemented in the software package Digimat®. The workflow contains five steps : 1) experimental campaign, 2) calibration of a mean-field homogenization model, 3) model reduction, 4) validation and 5) structural application.

The workflow has been applied to predict the failure of an injected beam with a Zytel® PA66GF30 composite produced by DuPont. Two material models have been presented. They are differentiated by the failure model used, a Tsai-Hill 3D transversely isotropic criteria at the pseudo-grain level on one side and a triaxiality based critical accumulated plastic strain on the other side. Both material models are able to capture the anisotropy shown in stiffness and in failure at various strain rate. The reduced model predicts the same behavior as the mean-field homogenization model on basic loading, except for in the transverse direction for aligned orientation. Both models accurately predict the nonlinear behavior of the beam.

The triaxiality based critical accumulated plastic strain criteria is promising since it reduces the gap between the displacement and force at break observed between the experimental data and the recommended Tsai-Hill 3D transversely isotropic criteria. Nevertheless, improvements are still needed, especially in the reduced model formulation, before the triaxiality model can become the recommended failure model.

## References

- [1] e-Xstream engineering, "Digimat documentation Release 2018.1," 2018, <http://www.e-xstream.com/>
- [2] I. Doghri and L. Tinel, "Micromechanical modeling and computation of elasto-plastic materials reinforced with distribution–orientation fibers", *Int J. Plasticity*, vol. 21, p. 1919-1940, 2005.
- [3] I. Doghri and C. Friebel, "Effective elasto-plastic properties of inclusion-reinforced composites. Study of shape, orientation and cyclic response", *Mech. Mater.*, vol 37, p. 46-68, 2005
- [4] S. Kammoun, I. Doghri, L. Adam, G. Robert and L. Delannay, "First pseudo-grain failure model for inelastic composites with misaligned fibers", *Composite Part A. : Applied Sciences and Manufacturing*, vol. 42, p. 1892-1902, 2011
- [5] Alan Wedgewood, Zhenyu Zhang and Thierry Malo, "Multi-Scale Modeling of an Injection Over-Molded Woven Fabric Beam", 2014 International SAMPE Symposium, Seattle WA, <https://www.nasampe.org/store/ListProducts.aspx?catid=439143&p=11>
- [6] Zhenyu Zhang, Alan Wedgewood and Helga Kuhlmann, "A Simulation Approach to Combine Multi-Scale Model Features with Failure at Composites Level for Short Fiber Reinforced Polymer", 2016 SIMULIA Community Conference, Boston MA, <http://www.3ds.com/events/science-in-the-age-of-experience>
- [7] A. Selmi, I. Doghri and L. Adam, "Micromechanical simulation of biaxial yield, hardening and plastic flow in short glass fiber reinforced polyamide", *Int. J. Mech. Sci.*, vol. 53, p. 696-706, 2011